

Granulysin Induces Cathepsin B Release from Lysosomes of Target Tumor Cells to Attack Mitochondria through Processing of Bid Leading to Necroptosis¹

Honglian Zhang, Chao Zhong, Lei Shi, Yuming Guo, and Zusen Fan²

Granulysin is a killer effector molecule localized in cytolytic granules of human NK and CTL cells. Granulysin exhibits broad antimicrobial activity and potent cytotoxic action against tumor cells. However, the molecular mechanism of granulysin-induced tumor lysis is poorly understood. In this study, we found that granulysin causes a novel cell death termed necroptosis. Granulysin can target lysosomes of target tumor cells and induce partial release of lysosomal contents into the cytosol. Relocalized lysosomal cathepsin B can process Bid to active tBid to cause cytochrome *c* and apoptosis-activating factor release from mitochondria. Cathepsin B silencing and Bid or Bax/Bak deficiency resists granulysin-induced cytochrome *c* and apoptosis-activating factor release and is less susceptible to cytolysis against target tumor cells. *The Journal of Immunology*, 2009, 182: 6993–7000.

Granule exocytosis-mediated cytolysis plays a major role in the innate and adaptive immunity against intracellular pathogens and tumor cells. Granulysin (GNLY)³ is colocalized in the cytotoxic granules along with a pore-forming protein, perforin (1, 2). GNLY has two major forms, 15 and 9 kDa. The 9-kDa form is processed from the larger precursor 15-kDa form and only the 9-kDa GNLY exerts cytolytic activity (3). GNLY is a member of the saposin-like protein family of lipid-binding proteins that includes amoebapores, saposins, and NK lysin (4–6). GNLY exhibits broad-spectrum antimicrobial activity against both Gram-positive and -negative bacteria, fungi, and parasites (7–9). Recent reports showed that cytotoxic CD8⁺ T cells and CD4⁺ T cells use GNLY, rather than perforin, to kill *Cryptococcus neoformans* (10, 11).

Besides its antimicrobial function, GNLY also harbors potent cytotoxic activity against tumor cells (12). GNLY can lyse Jurkat cells with apoptotic features in vitro. This apoptosis is associated with an increase of intracellular calcium and a decrease of intracellular potassium. Increasing intracellular calcium causes mitochondrial damage to release cytochrome *c* (cyt *c*) and apoptosis-inducing factor (AIF) leading to mitochondria-dependent cell death (13–17). Mitochondria-deficient RBC were not lysed by

GNLY even at a very high concentration. Krensky and colleagues (18) generated GNLY-transgenic mice and exhibited their significant protection against lethal tumor challenge. However, the molecular mechanism of GNLY-induced tumor lysis is less defined.

Lysosomes have been considered to be solely involved in necrotic and autophagic cell death for many years. Likewise, lysosomal proteases were believed to be limited to nonspecific intracellular protein degradation in the lysosome. However, recent accumulating evidence strongly demonstrated that lysosomes participate in the induction of apoptosis beyond that of simple “garbage disposals.” A complete destruction of lysosomes with release of high concentrations of lysosomal enzymes into the cytosol results in unregulated necrosis, whereas partial, sequential permeabilization triggers programmed cell death (PCD) (19). Several lysosomal proteases known as cathepsins, were released into the cytosol of target cells as a result of moderate lysosomal disruption (20, 21). Cathepsin B (Cath B) from lysosomes enhances mitochondrial release of cyt *c* and subsequent caspase activation in TNF-treated hepatocytes (22). Cathepsin D triggers Bax activation resulting in selective AIF release in T lymphocytes in the early commitment phase to apoptosis. An important cytosolic factor, Bid, was reported to be cleaved by some cathepsins and translocated to the mitochondria following lysosomal disruption by lysosomotropic agents (23). Thus, a lysosomal pathway is connected with a mitochondrial pathway to initiate apoptosis through these Bcl-2 family proteins. In this study, we found that GNLY can target lysosomes of target tumor cells and induce partial release of lysosomal contents. Relocalized lysosomal Cath B can process Bid to active tBid to cause cyt *c* and AIF release from mitochondria. Bid or Bak/Bax deficiency resists GNLY-induced cyt *c* and AIF release and necroptosis.

Materials and Methods

Cell lines, Abs, and reagents

Jurkat cells were grown in RPMI 1640 and HeLa cells in DMEM supplemented with 10% FCS, 50 μ M 2-ME, 100 U/ml penicillin, and 100 μ g/ml streptomycin. Mouse embryo fibroblasts (MEFs) were cultured in DMEM supplemented with 10% FCS, 100 μ M asparagine, and 50 μ M 2-ME. Bid wild-type (WT) MEFs and Bid knockout MEFs were provided by Dr. A. Strasser (The Walter and Eliza Hall Institute of Medical Research, Parkville, Australia) and Bax/Bak double knockout MEFs were provided by Dr. Q. Chen (Institute of Zoology, Chinese Academy of Sciences, Beijing, China). Human PBMC and RBC were obtained from healthy

National Laboratory of Biomacromolecules and Center for Infection and Immunity, Institute of Biophysics, Chinese Academy of Sciences, Beijing, China

Received for publication July 30, 2008. Accepted for publication March 20, 2009.

The costs of publication of this article were defrayed in part by the payment of page charges. This article must therefore be hereby marked *advertisement* in accordance with 18 U.S.C. Section 1734 solely to indicate this fact.

¹ This work was supported by the National Natural Science Foundation of China (Grants 30700126, 30772496, 30525005, and 30830030), 863 program (Grant 2006AA02Z4C9), 973 programs (Grants 2006CB504303 and 2006CB910901), the Innovative Program (KSCX2-YW-R-42), and the Hundred Talents Program of the Chinese Academy of Sciences.

² Address correspondence and reprint requests to Dr. Zusen Fan, National Laboratory of Biomacromolecules and Center for Infection and Immunity, Institute of Biophysics, Chinese Academy of Sciences, Beijing 100101, China. E-mail address: fanz@moon.ibp.ac.cn

³ Abbreviations used in this paper: GNLY, granulysin; cyt *c*, cytochrome *c*; Cath B, cathepsin B; MEF, mouse embryo fibroblast; STP, staurosporine; AO, acridine orange; AIF, apoptosis-inducing factor; PCD, programmed cell death; Z-RR-AMC, Z-Arg-Arg-7-amido-4-methylcoumarin hydrochloride; PI, propidium iodide; Z-FA-fmk, Z-Phe-Ala-fluoromethyl ketone; WT, wild type; shRNA, short hairpin RNA; CHX, cycloheximide.

Copyright © 2009 by The American Association of Immunologists, Inc. 0022-1767/09/\$2.00

volunteers and isolated by a lymphocyte separation kit. Commercial Abs were goat polyclonal to Cath B (Santa Cruz Biotechnology) for confocal and mouse anti-Cath B (Millipore) for Western blotting, rabbit polyclonal to LAMP-1 (Abcam), mouse anti-cyt c (BD Pharmingen), rabbit anti-AIF (BD Pharmingen), monoclonal anti- β -actin (Sigma-Aldrich), HRP-conjugated sheep anti-mouse IgG and HRP-conjugated sheep anti-rabbit IgG (Santa Cruz Biotechnology), Alexa Fluor 488-conjugated donkey anti-mouse IgG (Molecular Probes), and Alexa Fluor 594-conjugated donkey anti-rabbit IgG (Molecular Probes). Rabbit antiserum against Bid was provided by Dr. X. Wang (University of Texas Southwestern Medical Center, Dallas, TX) and mouse anti-GNLY was provided by Dr. A. Krensky (Stanford University, Stanford, CA). Propidium iodide (PI), acridine orange (AO), and Z-Arg-Arg-7-amido-4-methylcoumarin hydrochloride were obtained from Sigma-Aldrich. Mitotracker was from Molecular Probes. Z-FA-fmk and FITC-annexin V were purchased from BD Pharmingen.

Expression and purification of recombinant GNLY

pET28a-GNLY (a gift from A. Krensky) was expressed in *Escherichia coli* BL21-AI and the soluble supernatant was purified on a nickel column. Then the His tag was removed by thrombin treatment. Reverse-phase HPLC was used to further purification. After lyophilization, the protein was suspended in PBS. GNLY concentration was determined by the bicinchoninic acid assay (Pierce).

GNLY-mediated lysis of *Salmonella*

Lysis of *Salmonella* was measured as previously described (24). Briefly, a log-phase culture of *Salmonella* ($OD_{600} = 0.5$) was diluted to 2×10^5 /ml in 10 mM sodium phosphate buffer (pH7.4) containing 0.03% Luria-Bertani broth. Twenty-five-microliter aliquots of *Salmonella* were incubated with 25 μ l of different doses of recombinant GNLY at 37°C for 3 h. The mixture was diluted 100-fold with the cold phosphate buffer and plated on Luria-Bertani plates that were incubated at 37°C overnight. Bacterial colonies were counted.

Hemolytic assay

RBC of healthy volunteers were washed three times with PBS buffer. The washed RBC were suspended in PBS. Two percent RBC (v/v) were treated with GNLY at the indicated concentrations at 37°C for 4 h. H₂O-treated RBC were used as a positive control of complete hemolysis. Supernatant absorbance at 540 nm was measured for determination of hemolysis.

Electron microscopy

HeLa cells (1×10^6) were treated with GNLY at 37°C for 6 h. Cells were washed twice with PBS and fixed with 2% glutaraldehyde at 4°C for 1 h and postfixed with 2% osmium tetroxide. Cells were dehydrated with sequential washes in 50, 70, 80, 90, and 100% ethanol and then embedded in Spurr's resin. Ultrathin sections were obtained, mounted in copper grids, counterstained with uranyl acetate and lead citrate, and examined in a JEM-100 CX transmission electron microscopy.

DNA fragmentation assay

Jurkat (5×10^5) cells were treated with different doses of GNLY at 37°C for 6 h. Genomic DNA was extracted and analyzed by agarose gel electrophoresis.

DNA nicking assay

Jurkat or HeLa cells (2×10^5) cells were incubated with 50 μ M GNLY at 37°C for 6 h. The cells were harvested and washed twice with ice-cold PBS and resuspended in lysis buffer (20 mM Tris (pH 7.5), 0.5% Nonidet P-40, 25 mM KCl, and 5 mM MgCl₂). The nuclear pellet was harvested and incubated with 5 U of a Klenow fragment of DNA polymerase I and 10 μ Ci of [³²P]dATP at 37°C for 1 h. The nuclei were then washed completely and deproteinized for alkaline gel electrophoresis.

Laser-scanning confocal microscopy

HeLa cells were grown overnight to subconfluency at 37°C in 8-well chamber slides coated with rat collagen I (BD Falcon). Cells were treated with 50 μ M GNLY for the indicated times, washed, and fixed with 4% paraformaldehyde for 30 min at room temperature and permeabilized with 0.1% Triton X-100 for another 10 min, and the cells were incubated at room temperature for 1 h with anti-GNLY mAb and anti-LAMP-1 pAb (for Cath B release, incubated with anti-Cath B). The cells were further stained with Alexa Fluor 488-conjugated donkey anti-mouse IgG and Alexa Fluor 594-conjugated donkey anti-rabbit IgG. WT or Bid^{-/-} MEFs were grown overnight to subconfluency and incubated with 500 nM MitoTracker (Molec-

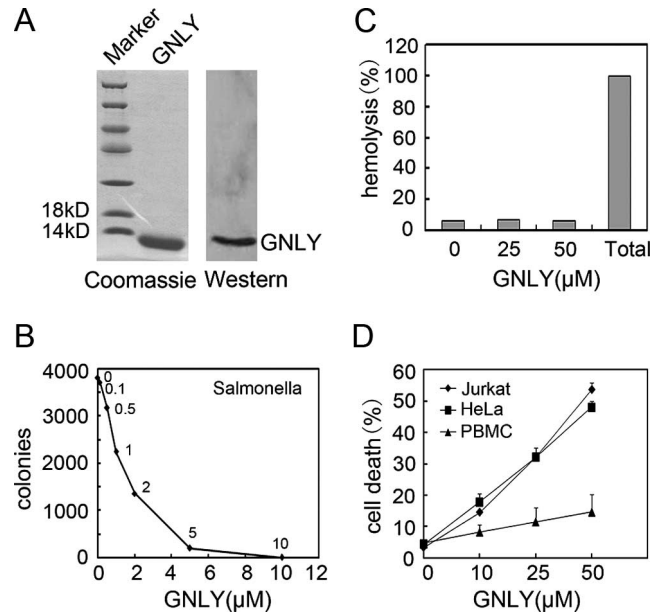


FIGURE 1. Recombinant GNLY possesses killing activity against *Salmonella* and target tumor cells. **A**, Purified recombinant GNLY protein was detected by Coomassie brilliant blue staining and Western blotting. **B**, Recombinant GNLY exhibits lytic activity against *Salmonella*. Bacterial colonies were counted after treatment by different doses of GNLY. **C**, Recombinant GNLY did not induce hemolysis of human RBC. Two percent RBC (v/v) were treated with GNLY at the indicated concentrations at 37°C for 4 h, and H₂O-treated cells were used as 100% hemolysis. **D**, GNLY showed similar killing activity against Jurkat and HeLa cells. Human PBMC were isolated from healthy human peripheral blood by a lymphocyte separation kit. Jurkat cells, HeLa cells, and PBMC were treated with different doses of GNLY for 6 h and stained by annexin V and PI. Data are representative of at least four separate experiments and are shown as mean \pm SD.

ular Probes) for 30 min. Cells were treated with 50 μ M GNLY for 1 h and probed with anti-cyt c mAb (clone 6H2.B4; BD Pharmingen). For the AO assay, HeLa cells were incubated with 5 μ g/ml AO in DMEM without serum at 37°C for 15 min and treated with 50 μ M GNLY for 6 h. The slides were observed using laser-scanning confocal microscopy (Olympus FV500 microscope).

Cellular Cath B activity assay

Cath B activity was measured as described elsewhere (25). Briefly, Jurkat cells were pretreated with the inhibitor Z-FA-fmk for 30 min before GNLY treatment. The treated cells were incubated with an extraction buffer (250 mM sucrose, 20 mM HEPES, 10 mM KCl, 1.5 mM MgCl₂, 1 mM EDTA, 1 mM EGTA, and 1 mM pefabloc, pH7.5) containing 15 μ g/ml digitonin for 15 min on ice. The total cellular Cath B activity was obtained by the extraction buffer containing 200 μ g/ml digitonin. The supernatants were added to 1 vol of 100 μ M Z-RR-AMC in cathepsin reaction buffer (50 mM sodium acetate, 4 mM EDTA, 8 mM DTT, and 1 mM pefabloc, pH 6.0). The mixture was incubated at 37 °C for 1 h. V_{max} of the liberation of amido-4-methylcoumarin hydrochloride (AMC) was measured through a fluorescence spectrophotometer F-4500.

Cleavage assay

GNLY-treated HeLa cells or Jurkat cells were lysed with 0.5% Nonidet P-40 lysis buffer and probed by anti-Bid Ab or caspase 3 for immunoblotting. In brief, 0.5 μ M rBid was incubated at 37°C for 2 h with different concentrations of Cath B in 20 μ l of cleavage buffer (50 mM sodium acetate, 4 mM EDTA, and 8 mM DTT, pH 7.0).

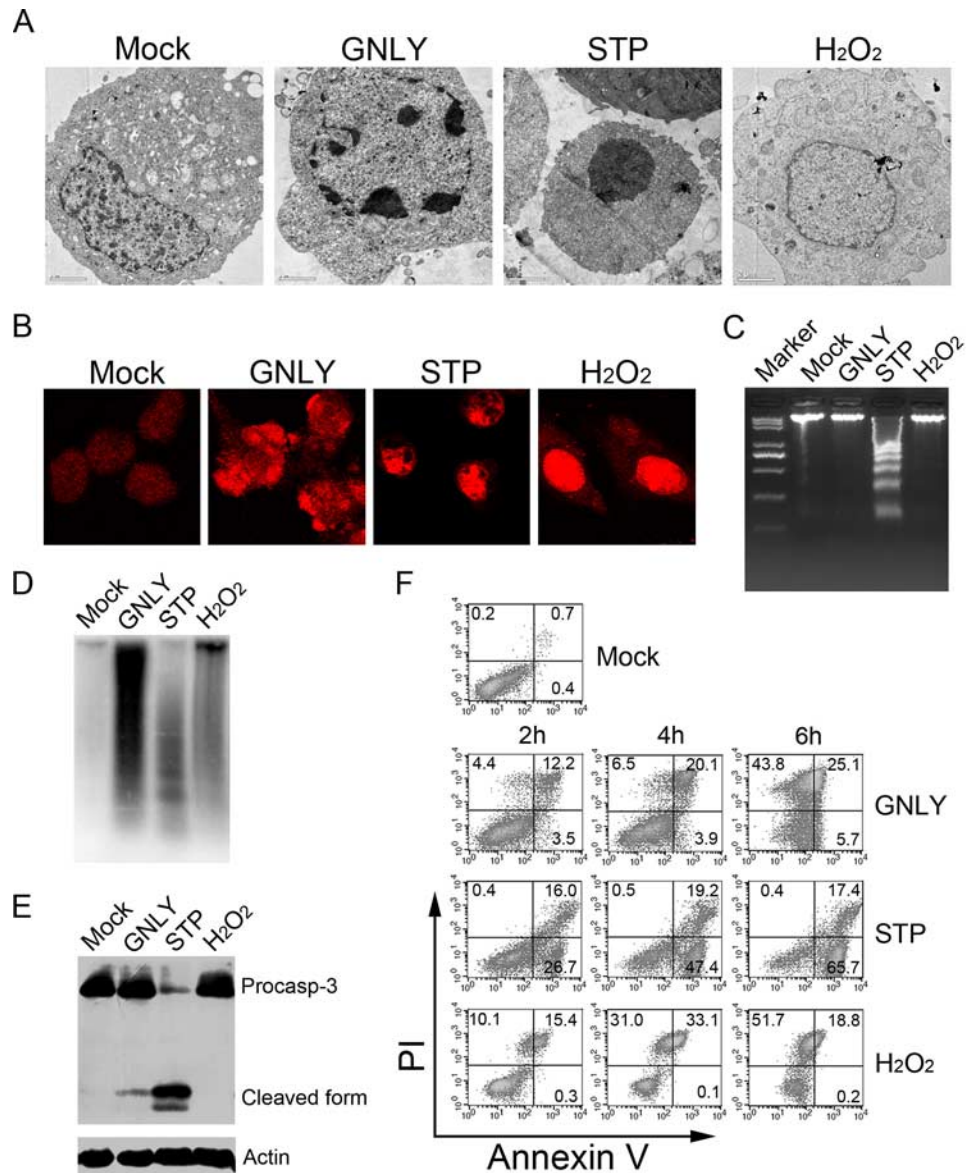
Flow cytometry analysis

Cells treated with GNLY were stained with annexin V and PI or PI alone and analyzed by flow cytometry using a FACSCalibur (BD Biosciences).

cyt c and AIF release assay

Cells (3×10^5) were treated with GNLY at the indicated times. Cells were washed twice with PBS and resuspended in 20 μ l of digitonin lysis buffer

FIGURE 2. GNLy induces necroptosis with ssDNA nicks. *A* and *B*, HeLa cells were incubated with 50 μ M GNLy or 10 μ g/ml STP or 20 mM H₂O₂ at 37°C for 6 h and detected by a high-magnification transmission electron microscopy (X1700) (*A*) or stained by PI and followed by confocal microscopy (*B*). *C*, GNLy does not cause dsDNA fragmentation. Jurkat cells were treated with 50 μ M GNLy or 10 μ g/ml STP or 20 mM H₂O₂ at 37°C for 6 h. Genomic DNA was extracted and visualized by 2% agarose gel electrophoresis with ethidium bromide staining. *D*, GNLy triggers ssDNA nicks. The nuclei of the above treated Jurkat cells were extracted and radiolabeled through Klenow DNA polymerase. The DNA nicks were detected by denaturing alkaline gel electrophoresis. *E*, Caspase 3 was less processed by GNLy. Jurkat cells (2×10^5) were treated as above and probed with anti-caspase 3 serum. β -Actin was unchanged as a loading control. *F*, Jurkat cells (2×10^5) cells were incubated with 50 μ M GNLy or 10 μ g/ml STP or 20 mM H₂O₂ at 37°C for the indicated times and stained by annexin V and PI. Data are representative at least three separate experiments.



(80 mM KCl, 250 mM sucrose, and 0.02% digitonin) for 5 min. The supernatants and the pellets were resolved on 12% SDS-PAGE and probed with cyt c or AIF Abs.

Cath B silencing, *Bid* silencing, and overexpression of *Bcl-2*

HeLa cells were transfected with pSUPER-siBid or pSUPER-LacZi plasmid (a gift from Dr. X. Jing, Cornell University Weill Graduate School of Medical Sciences, New York, NY) for Bid silencing control. pEF-Bcl-2 or pEF vector (a gift from Dr. A. Strasser, The Walter and Eliza Hall Institute of Medical Research, Parkville, Australia) was transfected for Bcl-2 overexpression. RNA sequences against Cath B for RNA interference were designed based on pSUPER system instructions (Oligoengine) and cloned into pSUPER-puro. Cath B short hairpin RNA (shRNA)-encoding sequences were as follows: sense, 5'-GAGCTACTTGAAGAGGCTA-3' and antisense, 5'-TAGCCTCTTCAAGTAGCTC-3'. HeLa cells were transfected by using Lipofectamine 2000 (Invitrogen) as described. Cath B-silenced, Bid-silenced, or Bcl-2 overexpressed stable cell lines were selected with puromycin.

Results

Recombinant GNLy possesses killing activity against Salmonella and target tumor cells

Recombinant 9-kDa GNLy was expressed in *E. coli* and purified by nickel affinity chromatography. The purified GNLy was deter-

mined with Coomassie brilliant blue staining and Western blotting (Fig. 1A). The recombinant GNLy showed strong killing activity to *Salmonella* in a dose-dependent manner (Fig. 1B), which is consistent with a previous report (25). Ten micromolar GNLy can completely inhibit the growth of 1×10^3 /ml *Salmonella*. In contrast, GNLy lacked lytic activity against RBC, even with a high dose of 50 μ M GNLy for 4 h (Fig. 1C). The results were in agreement with a previous observation (26). We also found the lytic effects of GNLy to human PBMC were comparable to the RBC (Fig. 1D). Previous studies demonstrated that GNLy induces cytolysis of Jurkat cells (13). In this study, we showed that GNLy can also kill HeLa cells with similar dynamics of those for Jurkat cells (Fig. 1D).

GNLy triggers necroptosis with ssDNA nicks

A previous report showed that GNLy induces nuclear morphology of typical apoptosis through staining with oxidized *p*-phenylenediamine (14). However, we found that GNLy-treated HeLa cells showed incomplete, lumpy chromatin condensation (Fig. 2A). These observed effects are consistent with cell death. PI staining exhibited similar morphological nuclear changes as shown in Fig.

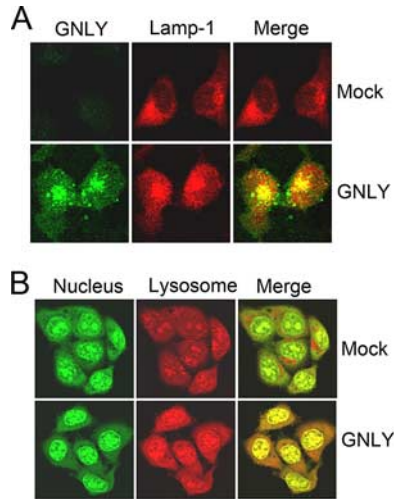


FIGURE 3. GNLY induces lysosomal membrane permeabilization. *A*, GNLY can target lysosomes of target cells. HeLa cells were treated with 50 μ M GNLY for 6 h and probed with anti-GNLY mAb and anti-LAMP-1 rabbit Ab, followed by staining with the second Alex Fluor 488-conjugated donkey anti-mouse Ab and Alex Fluor 594-conjugated donkey anti-rabbit Ab. GNLY staining green fluorescence is shown on the *left*, LAMP-1 staining red in the *middle*, and the merged image on the *right*. *B*, GNLY can trigger release of lysosomal contents into the cytosol. HeLa cells were incubated with AO and treated with 50 μ M GNLY for 6 h. AO shows green (nucleus and cytosol; *left*) and red (lysosome; *middle*). The merged image is on the *right*.

2B. These observations are unlike caspase-dependent strong chromatin compaction to crescent-shaped masses (27). Staurosporine (STP)-treated HeLa cells showed strong chromatin condensation as the apoptotic control (Fig. 2, *A* and *B*). Twenty micromolar H_2O_2 -treated cells had no apparent nuclear compaction as the necrotic control. To determine the form of DNA damage in GNLY-induced death, genomic DNA was extracted from GNLY-treated nuclei of Jurkat cells. Characteristic apoptotic DNA ladders were not visualized on agarose gels in GNLY-treated nuclei (Fig. 2*C*). H_2O_2 -treated nuclei did not show DNA ladders, while STP-treated cells exhibited typical DNA fragmentation. The DNA polymerase Klenow labeling was used to assess ssDNA breaks as previously described (28). GNLY caused increased [32 P]dATP incorporation and triggered ssDNA nicks (Fig. 2*D*). Although STP and H_2O_2 caused weak [32 P]dATP incorporation, STP-induced incorporation appeared to be DNA ladders. Caspase 3 activation is a key event in the induction of apoptosis. A previous report showed that caspase 3 was activated in GNLY-mediated cell death (15). However, we found that GNLY caused little caspase 3 processing (Fig. 2*E*). Most caspase 3 was activated in STP-treated cells, while H_2O_2 did not activate caspase 3. To further characterize the death features of GNLY-induced death, phosphatidylserine externalization was detected by using annexin V-FITC and PI staining. Phosphatidylserine externalization is an early hallmark of apoptosis. We found that GNLY-treated cells were both annexin V and PI positive even in early times (Fig. 2*F*). Most of the STP-treated cells were annexin V positive but PI negative. H_2O_2 -treated cells caused annexin V and PI double staining as expected for the necrotic control. Taken together, GNLY induces necroptosis with ssDNA nicks.

GNLY targets lysosomes of target tumor cells

GNLY is a saposin-like protein and interacts with lipids to cause the disruption of membranes. Lysosomes are an organelle with

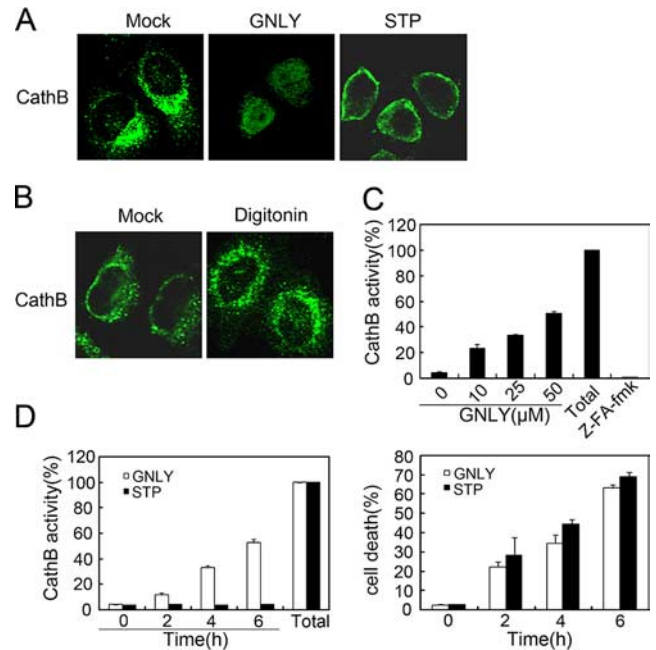


FIGURE 4. GNLY induces gradual release of Cath B from lysosomes. *A*, GNLY induces Cath B release to the cytosol. HeLa cells were treated with 50 μ M GNLY or STP and probed by anti-Cath B Ab. *B*, Digitonin (15 μ g/ml) did not induce Cath B relocation. HeLa cells were treated with 15 μ g/ml digitonin or mock treated and probed by anti-Cath B Ab. *C*, Cytosolic Cath B activity induced by GNLY is dose dependent. Jurkat cells (2×10^5) were treated with different doses of GNLY at 37°C for 6 h. The Cath B activity in the supernatant was detected by a fluorescence spectrophotometer. Two hundred micrograms of digitonin per ml of lysis buffer was used to lyse cells as total release. The cysteine protease pan inhibitor Z-FA-fmk can block Cath B activity. *D*, GNLY induced gradual release of Cath B from lysosomes. Jurkat cells (2×10^5) were treated with 50 μ M GNLY or STP at 37°C for the indicated times and analyzed Cath B activity (*left*) or the treated cells were stained with annexin V and PI for death analysis (*right*). These data represent at least four separate experiments.

lipid membranes. To determine whether GNLY enters into lysosomes of target cells, HeLa cells were treated with 50 μ M GNLY and probed by lysosome marker LAMP-1. We found that GNLY can get into the lysosomes of target cells (Fig. 3*A*). To further confirm the disruption of GNLY-induced lysosomal membrane, we detected its integrity by using a fluorogenic dye, AO. AO preferentially accumulates in acidic vesicles with a red fluorescence upon excitation with a blue light and it becomes a green fluorescence when it is presented in organelles of basic and neutral pH (29). After incubation with GNLY, lysosomal AO was released into the cytosol (Fig. 3*B*). Untreated HeLa cells showed a red fluorescence that was restricted to the lysosomal vesicles. These results indicate that GNLY induces the disruption of lysosomal membrane and releases the lysosomal contents to the cytoplasmic and nuclear compartments of target cells.

GNLY induces Cath B release from lysosomes

Cath B is the most abundant cysteine protease in the lysosome. A recent study reported that Cath B is associated with cell death induced by different death inducers (21). GNLY can destroy lysosome permeabilization and release lysosomal contents into the cytosol of target cells. To determine whether Cath B can release from lysosomes to the cytosol, HeLa cells were incubated with 50 μ M GNLY for 6 h and visualized by confocal microscopy. Cath B was in the perinuclear region localized in the lysosomes of untreated HeLa cells. However, its staining appeared diffuse throughout the

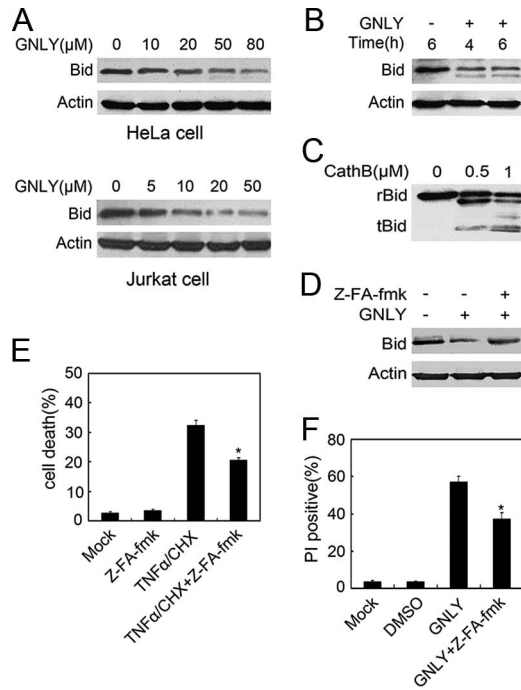


FIGURE 5. Bid can be processed by Cath B. *A* and *B*, Bid is cleaved in GNLly-treated target cells. HeLa cells or Jurkat cells (1×10^5) were treated with different doses of GNLly for 6 h (*A*) or HeLa cells with 50 μ M GNLly for the indicated times and probed with anti-Bid serum (*B*). β -Actin was unchanged as a loading control. *C*, Liver-purified Cath B can cleave Bid to tBid. In brief, 0.5 μ M rBid was treated with the indicated concentrations of Cath B at 37°C for 2 h in a neutral pH buffer. *D*, Z-FA-fmk can block Bid cleavage. HeLa cells were pretreated with 100 μ M Z-FA-fmk for 1 h before GNLly treatment. β -Actin was probed as a loading control. *E*, Z-FA-fmk decreases TNF- α /CHX-induced death. Jurkat cells (2×10^5) were pretreated with 100 μ M Z-FA-fmk for 60 min before 100 ng/ml TNF- α along with 10 μ g/ml CHX treatment and stained by annexin V and PI. Dead cells were calculated as double annexin V and PI and are shown as mean \pm SD. *, $p < 0.05$. *F*, Z-FA-fmk decreases GNLly-induced death. Jurkat cells (2×10^5) were pretreated with 100 μ M Z-FA-fmk for 30 min before GNLly treatment and stained by PI. The data represent at least four separate experiments. *, $p < 0.05$.

target cell after treatment by GNLly. STP did not cause the release of Cath B (Fig. 4*A*). Similar results were obtained for cathepsin L (data not shown). It indicates that GNLly initiates the release of lysosomal contents into the cytosol of target cells.

To quantitate the extent of lysosomal permeabilization, we measured the activity of Cath B in GNLly-treated cytosolic fractions through using the fluorescence substrate Z-RR-AMC. We detected that 15 μ g/ml digitonin extraction buffer was an optimal concentration for permeabilizing cell membranes without disruption of lysosomes (Fig. 4*B*). Approximately 10% of Cath B was released from the lysosome to the cytosol after GNLly treatment for 2 h. Cytosolic Cath B activity increased over time. About half of Cath B was released to the cytosol for 6 h or even longer. The cytosolic Cath B activity was measured in STP-treated cells as a control. Although the rates of cell death induced by 10 μ g/ml STP and 50 μ M GNLly were almost similar, the cytosolic Cath B activity treated by STP for 6 h was still very low (Fig. 4*D*). The release of Cath B from lysosomes induced by GNLly was in a dose-dependent manner (Fig. 4*C*). Cysteine protease pan inhibitor Z-FA-fmk (100 μ M) completely blocked Cath B activity. These confirm that GNLly triggers release of Cath B into the cytosol of target cells.

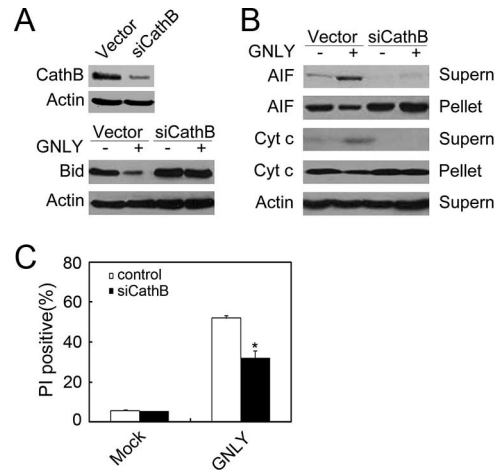


FIGURE 6. Cath B silencing reduces GNLly-mediated Bid processing and release of cyt c and AIF. *A*, Cath B silencing blocks GNLly-induced Bid processing. Cath B was silenced by transfection with pSUPER-Cath B-shRNA. β -Actin was a negative control. Cath B-silenced HeLa cells were treated with 50 μ M GNLly for 6 h and probed with anti-Bid serum. β -Actin was unchanged as a loading control. *B*, Cath B silencing reduces GNLly-induced release of cyt c and AIF. The supernatants and the pellets of target cells were separated after above treatment and detected by immunoblotting. *C*, Cath B silencing is resistant to GNLly-induced cell death. The above treated HeLa cells were stained by PI. PI-positive cells were calculated as mean \pm SD. *, $p < 0.05$. The data represent at least four separate experiments.

Cath B can process Bid to active tBid

Once Cath B was released from the lysosomes into the cytoplasm, it may cleave some target proteins to enhance cell death. A report showed that Cath B can cleave Bid to tBid at neutral pH *in vitro* (30). To determine whether Bid was degraded by GNLly, Bid was probed in GNLly-treated HeLa cells by anti-Bid Ab for immunoblotting. Bid was cleaved in a dose-dependent manner. Similar results were obtained in Jurkat cells (Fig. 5*A*). The cleaved products were undetectable maybe due to its low concentration or the Ab sensitivity. Bid was processed obviously within 4 h by GNLly treatment (Fig. 5*B*). β -Actin was probed as a loading control. To confirm that Cath B can process Bid at a neutral pH, rBid was treated with different concentrations of liver-purified Cath B at 37°C for 2 h in a cleavage buffer (pH 7.0). Cath B can directly cut rBid to produce an active 14-kDa tBid (Fig. 5*C*).

To evaluate whether released Cath B from the lysosome processes Bid, HeLa cells were pretreated with 100 μ M Z-FA-fmk for 30 min before incubation with GNLly. The cysteine protease pan inhibitor Z-FA-fmk blocked Bid degradation (Fig. 5*D*). One hundred micromolar Z-FA-fmk can partially inhibit TNF- α /cycloheximide (CHX)-induced cell death (Fig. 5*E*), which is in agreement with a previous report (31). To determine whether Cath B contributes to GNLly-induced death, Z-FA-fmk-pretreated HeLa cells were incubated with GNLly and followed by flow cytometry. Z-FA-fmk significantly blocked GNLly-induced death ($37.24 \pm 3.2\%$ vs $57.03 \pm 2.93\%$, $p < 0.01$; Fig. 5*F*).

Cath B silencing blocks GNLly-mediated Bid processing and release of cyt c and AIF

To confirm the role of Cath B in GNLly-mediated cell death, we designed shRNA sequences against Cath B and constructed pSUPER-Cath B-shRNA plasmid to silence Cath B expression. pSUPER-Cath B-shRNA stable cell lines were established by puromycin selection. Cath B was silenced as shown in Fig. 6*A*. β -Actin was

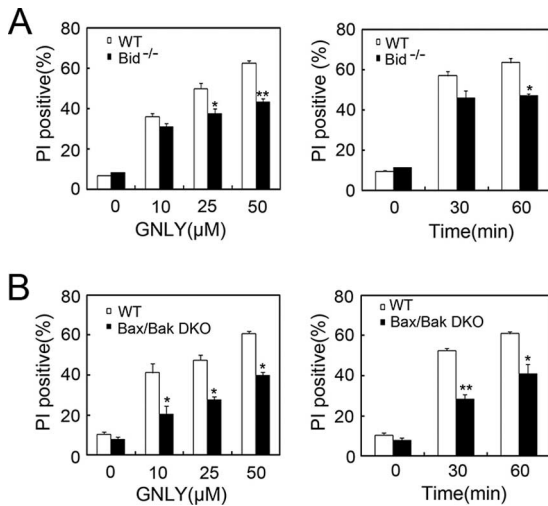


FIGURE 7. Bid knockout or Bax/Bak deficiency resists GNLY-induced death. *A*, Bid knockout MEFs reduced GNLY-induced death. WT or Bid^{-/-} MEFs were treated with different doses of GNLY for 1 h or 50 μM GNLY for the indicated times and stained by PI. *B*, Bax/Bak deficiency decreases GNLY-induced death. WT or Bax/Bak-deficient MEFs were treated as above. The data represent at least four separate experiments. *, $p < 0.05$ and **, $p < 0.01$.

unchanged as a control. Cath B-silenced and vector control-transfected HeLa cells were treated with GNLY at 37°C for 6 h. Cath B silencing blocked Bid degradation (Fig. 6*A*). Meanwhile, we found that Cath B silencing abolished GNLY-induced cyt c and AIF release (Fig. 6*B*). Moreover, Cath B-silenced HeLa cells were more resistant to GNLY-induced cytolysis compared with the vector control transfection (dead cells: $32 \pm 3.8\%$ vs $52 \pm 1.2\%$, $p < 0.01$; Fig. 6*C*). These results indicate that Cath B contributes to GNLY-mediated cell death.

Bid knockout or Bax/Bak-deficient MEFs decrease GNLY-induced death

To further determine whether Bid processing was associated with GNLY-induced death, Bid WT and knockout MEFs were treated with GNLY at 37°C for 1 h and stained with PI. Bid knockout MEFs were more resistant to GNLY-induced cytolysis. PI-positive cells in Bid WT and knockout MEFs were as follows (10 μM: $36.02 \pm 1.58\%$ vs $31.1 \pm 1.53\%$; 25 μM: $49.89 \pm 2.97\%$ vs $37.37 \pm 2.64\%$; and 50 μM: $62.64 \pm 1.24\%$ vs $43.29 \pm 1.55\%$; $p < 0.01$). Mock-treated cells got comparable background death (<10%). Time course experiments showed similar results to the above dose observations (Fig. 7*A*).

We next measured cell death of WT and Bax/Bak-deficient MEFs with the above-described GNLY treatment against Bid-deficient MEFs. Bax/Bak-deficient MEFs were still resistant to GNLY-induced death compared with WT MEFs (PI-positive cells: 10 μM, $20.28 \pm 4.25\%$ vs $41.13 \pm 4.56\%$; 25 μM: $27.49 \pm 1.76\%$ vs $47.56 \pm 2.38\%$; 50 μM: $39.71 \pm 1.63\%$ vs $60.76 \pm 1.08\%$; $p < 0.01$; Fig. 7*B*). Mock-treated cells obtained background death (<10%). Similar results were observed in a time course assay. These results demonstrate that GNLY-induced Bid processing utilizes the Bax/Bak pathway to target mitochondria.

Bid silencing or deficiency or Bcl-2 overexpression reduces GNLY-mediated cyt c and AIF release from mitochondria

To test whether Bid silencing affects GNLY-induced cyt c and AIF release, Bid was silenced in the human tumor cell line HeLa cells by transfection of pSUPER-siBid or a control nonsense *LacZ* se-

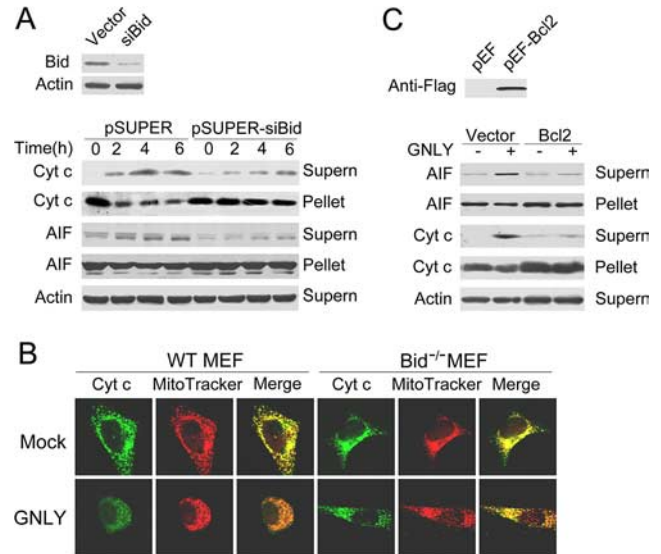


FIGURE 8. Bid silencing or knockout or Bcl-2 overexpression reduces GNLY-induced release of cyt c and AIF from mitochondria. *A*, Bid silencing decreases release of cyt c and AIF from mitochondria. Bid was silenced by transfection with pSUPER-Bid-shRNA. Bid-silenced HeLa cells were treated with 50 μM GNLY for the indicated times. The supernatants and the pellets of target cells were detected by immunoblotting. *B*, Bid deficiency reduces cyt c release from mitochondria through confocal microscopy. WT or Bid^{-/-} MEFs were treated with 50 μM GNLY for 1 h. cyt c green fluorescence is shown on the left, MitoTracker red in the middle, and the merged image on the right. *C*, Bcl-2 overexpression lowers release of cyt c and AIF from mitochondria. Bcl-2-overexpressed HeLa stable cell lines were obtained via transfection with pEF-FLAG-Bcl2 and selected by puromycin. Bcl-2-overexpressed HeLa cells were treated with 50 μM GNLY for 6 h and analyzed as above. The data represent at least three independent experiments.

quence plasmid pSUPER-*LacZ*. Bid-silenced stable cell lines were established by puromycin selection. Bid was almost undetectable through immunoblotting (Fig. 8*A*). Bid-silenced and control vector-transfected HeLa cells were treated with GNLY at 37°C at different time points. GNLY induced less cyt c and AIF release in Bid-silenced HeLa cells compared with those with transfection of the control vector (Fig. 8*A*). Similar results were achieved in Bid knockout MEFs (data not shown). These results were further confirmed by laser-scanning confocal microscopy. GNLY induced more cyt c release in WT MEFs than in Bid knockout MEFs (Fig. 8*B*). These data indicate that Bid processing can accelerate cyt c and AIF release into the cytosol of target cells.

Bcl-2 is an antiapoptotic protein in the Bcl-2 family. Bcl-2 suppresses apoptosis primarily by the inhibition of cyt c release. We wanted to look at whether Bcl-2 overexpression reduces cyt c and AIF release with GNLY treatment. pEF-Bcl-2 and a control empty vector plasmid were separately transfected into HeLa cells. Stable cell lines were established through puromycin selection. Bcl-2 was overexpressed in HeLa cells by immunoblotting with anti-Flag tag Ab (Fig. 8*C*). Bcl-2-overexpressed HeLa cells almost completely blocked the release of cyt c and AIF after GNLY treatment.

Discussion

PCD plays a very important role in the development, maintenance of multicellular organisms, and elimination of virally infected or transformed cells. Caspases have long been known as an essential role in apoptosis. Apoptosis is a kind of classical PCD, whose typical feature is the nuclear morphological changes with chromatin condensation and apparently simple geometric morphology

(globular, crescent shaped). During apoptosis, caspases, in particular caspase 3, are strongly activated and cause caspase-activated DNase activation resulting in dsDNA fragmentation. However, many studies reported that caspase inhibition does not prevent death-domain receptor-induced or granzyme A or K-induced cell death (32–34). Cell death induced by such conditions lacks the typical features of apoptosis, which is termed as necroptosis (35). In necroptosis, the nuclear morphological changes are not with obvious chromatin condensation, but with chromatin clustering to speckles. In this study, we found that GNLY-induced cell death as a type of necroptosis. GNLY-treated nuclei showed incomplete and lumpy chromatin condensation, but not strong chromatin compaction. On the other hand, although GNLY treatment also activates caspase 3, the level of caspase 3 activity was significantly lower than that in STP-treated cell death (Fig. 2E). We first defined the type of GNLY-induced death as necroptosis with ssDNA nicks, which is not consistent with a previous report for a typical apoptosis (14).

As reported, some necrotic PCD is often classified as “aborted apoptosis” that is initiated by a standard apoptosis program, then limited at the level of caspase activation and finally replaced by caspase-independent routes (36). Additionally, increasing Ca^{2+} and reactive oxygen species are also important inducers of necrotic PCD. A previous report showed that GNLY induces apoptosis of Jurkat cells associated with a dramatic increase of the ceramide: sphingomyelin ratio (14). Caspase pan inhibitor Z-VAD-fmk or ceramide synthase inhibitor cannot block GNLY-induced apoptosis. This suggests that GNLY induced death is through ceramide-independent or caspase-independent cell death pathways. An increased Ca^{2+} level in the cytoplasm precedes depolarization of mitochondria (13). Increasing Ca^{2+} triggers loss of mitochondrial potential and release of cyt c and AIF. However, procaspase 9 is not processed to its active form in GNLY-induced death. Therefore, GNLY induces a novel death pathway whose mechanism is poorly understood.

GNLY belongs to the saposin-like protein family of lipid-binding proteins that interacts with cell membranes of target cells. Recently, Ziegler and colleagues (37, 38) found that the cholesterol content is very important for GNLY to destroy intracellular bacteria without damaging the infected cells. The content of cholesterol in the cell membrane of bacteria is low; therefore, it is very susceptible to GNLY. Another study (39) reported that cholesterol is enriched in the plasma membrane and in membranes of early endocytic organelles but it is nearly completely absent in inner lysosomal membranes. Surprisingly, we found that GNLY can enter into lysosomes and induce lysosomal contents release into the cytosol of target cells. The release of lysosomal contents is limited and partial. This result is consistent with the dynamic process of GNLY-induced necroptosis.

Lysosomal cysteine proteases termed cathepsins represent the largest group of proteolytic enzymes in the lysosomes. Cath B and cathepsin L are the most abundant in the lysosomes. Cathepsins have been implicated in the induction of apoptosis (40). Cath B-deficient hepatocytes are resistant to TNF-mediated apoptosis and mitochondrial release of cyt c. Cath B participates in caspase-independent cell death of WEHI-S cells (31). Bid activation may be a direct link between cathepsins and mitochondrial damage. Bid can be processed to active form by Cath B and cause cyt c release from mitochondria (19). Moreover, Cath B is more stable at physiological pH and less effectively inhibited by the major endogenous cysteine inhibitor cystatin B. Therefore, Cath B might play a critical role in lysosome-mediated Bid activation. In this study, we found that Cath B releases into the cytosol of target cells and Bid processing occurs with GNLY treatment. The cysteine protease

pan inhibitor Z-FA-fmk can block Bid cleavage in GNLY-treated target cells, leading to a decrease in cell death. Moreover, Cath B silencing blocks Bid processing and releasing of cyt c and AIF from the mitochondria. Cath B-silenced HeLa cells are resistant to GNLY-induced cell death. These data suggest that Bid may be processed by Cath B to initiate mitochondrial dysfunction.

Proapoptotic Bcl-2 proteins such as Bax/Bak induce a selective process of outer membrane permeabilization of mitochondria through the formation of channels or pores that allow the selective release of proteins soluble in the inner membrane space like cyt c. We found that Bid knockout or Bax/Bak deficiency indeed resists release of cyt c and AIF to decrease GNLY-induced death. This indicates that GNLY-mediated mitochondrial damage is Bid dependent. Bid knockout or Bax/Bak deficiency partially lowers GNLY-induced death. These results imply that other pathways involve this process such as increase of intracellular Ca^{2+} . In this study, we first demonstrated that GNLY can target lysosomes to release Cath B, leading to Bid cleavage. Bid activation may be a direct link between cathepsin release and mitochondrial dysfunction in GNLY-induced necroptosis.

Acknowledgments

We thank Y. Teng, C. C. Liu, and L. Sun for their technical support and thank Drs. A. Krensky, A. Strasser, X. Wang, Q. Chen, D. Green, and X. Jiang for providing reagents and materials.

Disclosures

The authors have no financial conflict of interest.

References

- Fan, Z., and Q. X. Zhang. 2005. Molecular mechanisms of lymphocyte-mediated cytotoxicity. *Cell. Mol. Immunol.* 2: 259–264.
- Russell, J. H., and T. J. Ley. 2002. Lymphocyte-mediated cytotoxicity. *Annu. Rev. Immunol.* 20: 323–370.
- Hanson, D. A., A. A. Kaspar, F. R. Poulain, and A. M. Krensky. 1999. Biosynthesis of granulysin, a novel cytolytic molecule. *Mol. Immunol.* 36: 413–422.
- Leippe, M., S. Ebel, O. L. Schoenberger, R. D. Horstmann, and H. J. Muller-Eberhard. 1991. Pore-forming peptide of pathogenic *Entamoeba histolytica*. *Proc. Natl. Acad. Sci. USA* 88: 7659–7663.
- Munford, R. S., P. O. Sheppard, and P. J. O'Hara. 1995. Saposin-like proteins (SAPLIP) carry out diverse functions on a common backbone structure. *J. Lipid Res* 36: 1653–1663.
- Andersson, M., H. Gunne, B. Agerberth, A. Boman, T. Bergman, R. Sillard, H. Jornvall, V. Mutt, B. Olsson, H. Wigzell, et al. 1995. NK-lysin, a novel effector peptide of cytotoxic T and NK cells: structure and cDNA cloning of the porcine form, induction by interleukin 2, antibacterial and antitumour activity. *EMBO J.* 14: 1615–1625.
- Ochoa, M. T., S. Stenger, P. A. Sieling, S. Thoma-Uszynski, S. Sabet, S. Cho, A. M. Krensky, M. Rollinghoff, E. Nunes Sarno, A. E. Burdick, et al. 2001. T-cell release of granulysin contributes to host defense in leprosy. *Nat. Med.* 7: 174–179.
- Ma, L. L., C. L. Wang, G. G. Neely, S. Epelman, A. M. Krensky, and C. H. Mody. 2004. NK cells use perforin rather than granulysin for anticryptococcal activity. *J. Immunol.* 173: 3357–3365.
- da Silva, A. P., D. Unks, S. C. Lyu, J. Ma, R. Zboznic-Pacamaj, X. Chen, A. M. Krensky, and C. Clayberger. 2008. In vitro and in vivo antimicrobial activity of granulysin-derived peptides against *Vibrio cholerae*. *J. Antimicrob. Chemother.* 61: 1103–1109.
- Ma, L. L., J. C. Spurrell, J. F. Wang, G. G. Neely, S. Epelman, A. M. Krensky, and C. H. Mody. 2002. CD8 T cell-mediated killing of *Cryptococcus neoformans* requires granulysin and is dependent on CD4 T cells and IL-15. *J. Immunol.* 169: 5787–5795.
- Zheng, C. F., G. J. Jones, M. Shi, J. C. Wiseman, K. J. Marr, B. M. Berenger, S. M. Huston, M. J. Gill, A. M. Krensky, P. Kubes, and C. H. Mody. 2008. Late expression of granulysin by microbicidal CD4⁺ T cells requires PI3K- and STAT5-dependent expression of IL-2R β that is defective in HIV-infected patients. *J. Immunol.* 180: 7221–7229.
- Pena, S. V., D. A. Hanson, B. A. Carr, T. J. Goraliski, and A. M. Krensky. 1997. Processing, subcellular localization, and function of 519 (granulysin), a human late T cell activation molecule with homology to small, lytic, granule proteins. *J. Immunol.* 158: 2680–2688.
- Clayberger, C., and A. M. Krensky. 2003. Granulysin. *Curr. Opin. Immunol.* 15: 560–565.
- Gamen, S., D. A. Hanson, A. Kaspar, J. Naval, A. M. Krensky, and A. Anel. 1998. Granulysin-induced apoptosis: I. Involvement of at least two distinct pathways. *J. Immunol.* 161: 1758–1764.

15. Kaspar, A. A., S. Okada, J. Kumar, F. R. Poulain, K. A. Drouvalakis, A. Kelekar, D. A. Hanson, R. M. Kluck, Y. Hitoshi, D. E. Johnson, et al. 2001. A distinct pathway of cell-mediated apoptosis initiated by granulysin. *J. Immunol.* 167: 350–356.
16. Pardo, J., P. Perez-Galan, S. Gamen, I. Marzo, I. Monleon, A. A. Kaspar, S. A. Susin, G. Kroemer, A. M. Krensky, J. Naval, and A. Anel. 2001. A role of the mitochondrial apoptosis-inducing factor in granulysin-induced apoptosis. *J. Immunol.* 167: 1222–1229.
17. Okada, S., Q. Li, J. C. Whitin, C. Clayberger, and A. M. Krensky. 2003. Intracellular mediators of granulysin-induced cell death. *J. Immunol.* 171: 2556–2562.
18. Huang, L. P., S. C. Lyu, C. Clayberger, and A. M. Krensky. 2007. Granulysin-mediated tumor rejection in transgenic mice. *J. Immunol.* 178: 77–84.
19. Guicciardi, M. E., M. Leist, and G. J. Gores. 2004. Lysosomes in cell death. *Oncogene* 23: 2881–2890.
20. Werneburg, N. W., M. E. Guicciardi, S. F. Bronk, S. H. Kaufmann, and G. J. Gores. 2007. Tumor necrosis factor-related apoptosis-inducing ligand activates a lysosomal pathway of apoptosis that is regulated by Bcl-2 proteins. *J. Biol. Chem.* 282: 28960–28970.
21. Yeung, B. H., D. C. Huang, and F. A. Sinicrope. 2006. PS-341 (bortezomib) induces lysosomal cathepsin B release and a caspase-2-dependent mitochondrial permeabilization and apoptosis in human pancreatic cancer cells. *J. Biol. Chem.* 281: 11923–11932.
22. Guicciardi, M. E., J. Deussing, H. Miyoshi, S. F. Bronk, P. A. Svingen, C. Peters, S. H. Kaufmann, and G. J. Gores. 2000. Cathepsin B contributes to TNF- α -mediated hepatocyte apoptosis by promoting mitochondrial release of cytochrome c. *J. Clin. Invest.* 106: 1127–1137.
23. Bidere, N., H. K. Lorenzo, S. Carmona, M. Laforge, F. Harper, C. Dumont, and A. Senik. 2003. Cathepsin D triggers Bax activation, resulting in selective apoptosis-inducing factor (AIF) relocation in T lymphocytes entering the early commitment phase to apoptosis. *J. Biol. Chem.* 278: 31401–31411.
24. Wang, Z., E. Choice, A. Kaspar, D. Hanson, S. Okada, S. C. Lyu, A. M. Krensky, and C. Clayberger. 2000. Bactericidal and tumoricidal activities of synthetic peptides derived from granulysin. *J. Immunol.* 165: 1486–1490.
25. Nylandsted, J., M. Gyrd-Hansen, A. Danielewicz, N. Fehrenbacher, U. Lademann, M. Hoyer-Hansen, E. Weber, G. Multhoff, M. Rohde, and M. Jaattela. 2004. Heat shock protein 70 promotes cell survival by inhibiting lysosomal membrane permeabilization. *J. Exp. Med.* 200: 425–435.
26. Li, Q., C. Dong, A. Deng, M. Katsumata, A. Nakadai, T. Kawada, S. Okada, C. Clayberger, and A. M. Krensky. 2005. Hemolysis of erythrocytes by granulysin-derived peptides but not by granulysin. *Antimicrob. Agents Chemother.* 49: 388–397.
27. Leist, M., and M. Jaattela. 2001. Four deaths and a funeral: from caspases to alternative mechanisms. *Nat. Rev. Mol. Cell Biol.* 2: 589–598.
28. Fan, Z., P. J. Beresford, D. Y. Oh, D. Zhang, and J. Lieberman. 2003. Tumor suppressor NM23-H1 is a granzyme A-activated DNase during CTL-mediated apoptosis, and the nucleosome assembly protein SET is its inhibitor. *Cell* 112: 659–672.
29. Barbosa, C. M., C. R. Oliveira, F. D. Nascimento, M. C. Smith, D. M. Fausto, M. A. Soufen, E. Sena, R. C. Araujo, I. L. Tersariol, C. Bincoletto, and A. C. Caires. 2006. Biphosphinic palladacycle complex mediates lysosomal-membrane permeabilization and cell death in K562 leukaemia cells. *Eur. J. Pharmacol.* 542: 37–47.
30. Cirman, T., K. Oresic, G. D. Mazovec, V. Turk, J. C. Reed, R. M. Myers, G. S. Salvesen, and B. Turk. 2004. Selective disruption of lysosomes in HeLa cells triggers apoptosis mediated by cleavage of Bid by multiple papain-like lysosomal cathepsins. *J. Biol. Chem.* 279: 3578–3587.
31. Foghsgaard, L., D. Wissing, D. Mauch, U. Lademann, L. Bastholm, M. Boes, F. Elling, M. Leist, and M. Jaattela. 2001. Cathepsin B acts as a dominant execution protease in tumor cell apoptosis induced by tumor necrosis factor. *J. Cell Biol.* 153: 999–1010.
32. Holler, N., R. Zaru, O. Micheau, M. Thome, A. Attinger, S. Valitutti, J. L. Bodmer, P. Schneider, B. Seed, and J. Tschopp. 2000. Fas triggers an alternative, caspase-8-independent cell death pathway using the kinase RIP as effector molecule. *Nat. Immunol.* 1: 489–495.
33. Lieberman, J., and Z. Fan. 2003. Nuclear war: the granzyme A-bomb. *Curr. Opin. Immunol.* 15: 553–559.
34. Zhao, T., H. Zhang, Y. Guo, Q. Zhang, G. Hua, H. Lu, Q. Hou, H. Liu, and Z. Fan. 2007. Granzyme K cleaves the nucleosome assembly protein SET to induce single-stranded DNA nicks of target cells. *Cell Death Differ.* 14: 489–499.
35. Degtarev, A., Z. Huang, M. Boyce, Y. Li, P. Jagtap, N. Mizushima, G. D. Cuny, T. J. Mitchison, M. A. Moskowitz, and J. Yuan. 2005. Chemical inhibitor of nonapoptotic cell death with therapeutic potential for ischemic brain injury. *Nat. Chem. Biol.* 1: 112–119.
36. Nicotera, P., M. Leist, and L. Manzo. 1999. Neuronal cell death: a demise with different shapes. *Trends Pharmacol. Sci.* 20: 46–51.
37. Barman, H., M. Walch, S. Latinovic-Golic, C. Dumrese, M. Dolder, P. Groscurth, and U. Ziegler. 2006. Cholesterol in negatively charged lipid bilayers modulates the effect of the antimicrobial protein granulysin. *J. Membr. Biol.* 212: 29–39.
38. Walch, M., E. Eppler, C. Dumrese, H. Barman, P. Groscurth, and U. Ziegler. 2005. Uptake of granulysin via lipid rafts leads to lysis of intracellular *Listeria innocua*. *J. Immunol.* 174: 4220–4227.
39. Kolter, T., and K. Sandhoff. 2005. Principles of lysosomal membrane digestion: stimulation of sphingolipid degradation by sphingolipid activator proteins and anionic lysosomal lipids. *Annu. Rev. Cell Dev. Biol.* 21: 81–103.
40. Ferri, K. F., and G. Kroemer. 2001. Organelle-specific initiation of cell death pathways. *Nat. Cell Biol.* 3: E255–E263.